

# Effects of Screening on Quark-Antiquark Cross Sections in Quark-Gluon Plasma

Cheuk-Yin Wong<sup>1</sup> and Lali Chatterjee<sup>1,2</sup>

<sup>1</sup>Oak Ridge National Laboratory, Oak Ridge, TN 37831

<sup>2</sup>Department of Physics, University of Tennessee, Knoxville, TN 37996

(March 1, 2022)

## Abstract

Lowest-order cross sections for  $q\bar{q}$  production and annihilation can be approximately corrected for higher-order QCD effects by using a corrective  $K$ -factor. For energies where quark masses cannot be ignored, the  $K$ -factor is dominated by the wave function distortion arising from the initial- or final-state interaction between the quark and the antiquark. We evaluate this  $K$ -factor for  $q\bar{q}$  production and annihilation in a quark-gluon plasma by taking into account the effects of Debye screening through a color-Yukawa potential. We present the corrective  $K$ -factor as a function of dimensionless parameters which may find applications in other systems involving attractive or repulsive Yukawa interactions. Prominent peaks of the  $K$ -factor occur for an attractive  $q\bar{q}$  color-Yukawa interaction with Debye screening lengths of 0.835 and 3.23 times the Bohr radius, corresponding to two lowest  $s$ -wave  $q\bar{q}$  bound states moving into the continuum to become  $q\bar{q}$  resonances as the Debye screening length decreases. These resonances, especially the  $c\bar{c}$  and the  $b\bar{b}$  resonances, may be utilized to search for the quark-gluon plasma by studying the sys-

tem atics of the tem perature dependence of heavy-quark pair production just above the threshold.

PAC S num ber(s): 25.75.+ r, 24.85.+ p, 12.38 M h, 13.90.+ i

## I. INTRODUCTION AND SUMMARY

The possible production of a deconfined quark-gluon plasma (QGP) state during high-energy heavy-ion collisions [1{7] is expected to be accompanied by Debye screening of the color charges of the constituents in the plasma [8{10,2]. The nature and the characteristics of the screening depend on the degree of equilibration and the condition of the plasma. Lattice QCD calculations also provide information on the extent of color screening [10]. While the actual temperatures that might be attained cannot be conclusively established at the present state of the art, reasonable estimates of the temperature and other plasma properties have been made for different scenarios and for different experimental conditions [11{13]. On the basis of these, corresponding estimates can be made for the color screening that would be operative for various scenarios. Recent phenomenology of soft-particle production [14,15] and the "hot glue" partons scenario [12], suggesting a possible initial gluon-rich environment in nucleus-nucleus collisions, raise additional questions regarding color screening in gluon-rich matter as well.

The screening phenomenon modifies the interaction between a quark and an antiquark placed in the medium and affects their rates of production and annihilation. Many of these reactions, such as the electromagnetic annihilation of  $q\bar{q}$  pairs and the production of strange and charm quark pairs from the plasma, provide valuable signals for the presence of the plasma [1{7]. It is clearly important to understand the influence of a screened color interaction on various cross sections.

It is well known that the lowest-order  $q\bar{q}$  annihilation and production cross sections need to be corrected to take into account initial-state and final-state interactions. At high energies, a  $K$ -factor is used to correct the tree-level rates to achieve a match with experiments [16{20]. At relatively low energies near the  $q\bar{q}$  threshold, the importance of the final-state interaction on the production of heavy quarks has been recognized by many authors [21{26]. Similar effects of initial- and final-state interactions have also been recognized in many other areas of physics [27{30]. The Gamow factor (in nuclear reactions [27], pion production and pion

interferometry [28], and pair annihilations [29]) and the  $F$ -factor (in nuclear beta decay [30]) have been successfully utilized to correct the lowest-order reaction cross sections or decay rates. For example, in beta-decay, the probability for the occurrence of low-energy electrons is greatly enhanced because of the attractive final-state Coulomb interaction between the electron and the nuclear charge, while the probability for the emission of low-energy positrons is suppressed by the repulsive final-state Coulomb interaction. The corrective factors can be numerically quite different from unity, especially at energies only slightly greater than the rest masses of reacting participants.

We have in an earlier work presented an approximate representation for the  $K$ -factor to correct lowest-order  $q\bar{q}$  cross sections to take into account the initial- and final-state color-Coulomb interaction without screening [31]. At energies where quark masses are important, we have determined the  $K$ -factor by the wave function distortion effects resulting from the color-Coulomb interaction between the quark and the antiquark. For the relativistic case at very high energies, the corrective  $K$ -factor has been determined from perturbative quantum chromodynamics (PQCD) [16{19]. Our approximate representation of the corrective  $K$ -factor for the case of no screening interpolates between the low- and the high-energy limits, following the interpolation procedure of Schwinger [32]. It has been tested and found to give a good description of the E605 data on dilepton production in the Drell-Yan process [33] and the experimental ratio of  $(e^+e^- \rightarrow \text{hadrons})/(e^+e^- \rightarrow \mu^+\mu^-)$  [34].

In this work we evaluate the  $K$ -factor by including the effects of screening arising from the consideration of wave function distortion only. As these corrections are most important at low energies, we restrict our investigation to non-relativistic equations of motion at present. In future work, we hope to examine the relativistic case where the relative energy is much greater than the quark masses.

Attractive and repulsive Yukawa potentials appear in many other areas of physics. To make the corrective  $K$ -factor obtained here useful also for reactants in any attractive or repulsive Yukawa potential, we present the corrective factor as a function of two dimensionless parameters. For attractive screened interactions, we observe interesting peaks of the

$K$ -factor as a function of the screening length, which correspond to single-particle  $q\bar{q}$  bound states moving into the continuum as the screening length decreases. These peaks occur when the Debye screening length  $\lambda_D$  is equal to 0.835 and 3.23 times the Bohr radius  $a_B$ .

The phase shifts and scattering cross sections for the attractive screened Coulomb potential have been evaluated earlier by Morse and his collaborator for the scattering of electrons from an atom [35,36] and also by Calogero [37]. By comparing our  $K$ -factor results with the phase shifts of Morse and collaborators, we found that the  $s$ -wave resonances at  $E = 0$  occur at the same ratios of  $\lambda_D = a_B$  as the peaks of the  $K$ -factor. Therefore, the occurrence of the peaks of the  $K$ -factor and the resonances at  $E = 0$  are the manifestations of the same physical phenomenon arising from emergence of the single-particle  $q\bar{q}$  bound states into the continuum to become  $q\bar{q}$  resonances. Because they arise from Debye screening in a deconfined quark-gluon plasma at high temperatures, they can be called "screening resonances" to be distinguished from other usual  $q\bar{q}$  resonances such as  $J = 0, 1, 2$ , and  $3$  in the confining phase.

The occurrence of the  $q\bar{q}$  screening resonances, especially the  $c\bar{c}$  and the  $b\bar{b}$  screening resonances, may provide a way to search for the quark-gluon plasma. Because the screening length is inversely proportional to the temperature, the peaks in the  $K$ -factor will appear at specific values of the temperature. Therefore, very large enhancement of the production of  $c\bar{c}$  or  $b\bar{b}$  pairs near the thresholds will occur at the corresponding temperatures specified by the resonance screening length parameter. A systematic study of the dependence of the  $K$ -factor for heavy-quark pair production near the threshold as a function of temperature will be useful to map out the effect of screening, which will identify important characteristics of the deconfined quark-gluon plasma.

This paper is organized as follows. In Section II, we discuss the phase-amplitude method to calculate the  $K$ -factor for a screened Coulomb-type potential. The corrective  $K$ -factor is calculated for attractive and repulsive potentials and the results are exhibited in Section III as a function of two dimensionless parameters. In Section IV, we calculate the  $K$ -factors for charm and strange pair production in a quark-gluon plasma. We show how the screening

modifies the lowest-order cross sections for  $ss$  and  $cc$  production in Section V. Section VI summarizes the present investigation and discusses how the  $qq$  resonances in the deconfined phase may be used to search for the quark-gluon plasma.

## II. THE K-FACTOR FOR SCREENED COLOR POTENTIAL

Basic processes involving  $q$ - $q$  initial-state or final-state interactions include dilepton production through  $qq \rightarrow \ell\ell$ , charm and strange pair production through  $qq \rightarrow g \rightarrow qq$  ( $ss; cc$ ) and  $gg \rightarrow qq$  ( $ss; cc$ ).

In the lowest-order reaction cross sections for these processes, the quark and the antiquark are described by plane waves, and their mutual initial- or final-state interactions are not included. The quark and the antiquark however interact with each other through a color-Coulomb strong interaction, with a large coupling constant. While one can obtain the effect of these interactions to the next order in perturbation theory, there are situations in which a perturbation expansion involving only the lowest two orders may not be sufficient, as in the case of large coupling constants and at energies where the quark masses are not negligible. A nonperturbative correction, based on the use of the distorted wave function in the presence of the color-Coulomb potential, can provide non-perturbative corrections to the cross sections [23, 26, 31].

If one places a quark and an antiquark in a color medium such as a quark-gluon plasma or gluon-rich matter, the interaction between the quark and the antiquark will be screened. In the case of a quark-gluon plasma, the degree of screening depends on the temperature. The greater the temperature, the greater the density of quarks, antiquarks, and gluons, and the greater will be the degree of screening. The effects of Debye screening in the quark-gluon plasma will modify the configuration space representation of the virtual gluon propagator between the quark and the antiquark. The color potential connecting the quark and the antiquark will be modified from a color-Coulomb interaction into a color-Yukawa interaction. (For an introduction, see page 349 of Ref. [2].) The screened interaction will modify the

quark-antiquark relative wave function, and will therefore change the corrective  $K$ -factor which is given by the square of the wave-function at contact. We therefore need to evaluate the wave function for a quark and an antiquark in a screened color potential.

The  $q\bar{q}$  Schrodinger equation in the relative coordinate  $r$  can be written as

$$[\nabla^2 + k^2 - 2V(r)]\psi(r) = 0; \quad (1)$$

where  $\mu$  is the reduced mass, and the wave number  $k$  at infinite separation is related to the nonrelativistic kinetic energy  $E$  by  $k^2 = 2\mu E$ . The screened color potential  $V(r)$  which describes the interaction between the quark and the antiquark can be written as [2,8,9]

$$V(r) = -\frac{e^2 e^{-r/\lambda_D}}{r}; \quad (2)$$

where the Debye screening length  $\lambda_D$  is inversely proportional to quark-gluon plasma temperature  $T$  [38], and the effective coupling constant  $e^2$  is related to the strong coupling  $g_s^2$  by the color factor  $C_f$ :

$$e^2 = C_f g_s^2; \quad (3)$$

We have included a negative sign on the righthand side of the potential (2). Thus, when  $q$  and  $\bar{q}$  are in a color-singlet state,  $C_f$  is  $4/3$  [18],  $e^2$  is positive, and the interaction is attractive. When  $q$  and  $\bar{q}$  are in a color-octet state,  $C_f$  is  $-1/6$  [18],  $e^2$  is negative, and the interaction is repulsive.

Following Calogero [37], we use the phase-amplitude method to solve the Schrodinger equation for the  $s$ -state. We write the  $s$ -wave radial wave function  $u_0(r) = r\psi(r)$  in terms of the phase shift function  $\delta_0(r)$  and the amplitude function  $\rho_0(r)$  as

$$u_0(r) = \rho_0(r) \cos[\delta_0(r) - kr] = \rho_0(r) \sin(kr + \delta_0(r)); \quad (4)$$

From the Schrodinger equation (1), the equation for the  $s$ -wave phase shift function  $\delta_0(r)$  is [37]

$$\frac{d\delta_0(r)}{dr} = -k \left[ 1 - 2V(r) \sin^2[kr + \delta_0(r)] \right]; \quad (5)$$

This is a first-order differential equation which can be solved numerically starting from the origin, with the boundary condition  $\psi_0(0) = 0$ . After the function  $\psi_0(r)$  is determined, the amplitude function  $\psi_0(r)$  can be obtained from the relation [37]

$$\psi_0(r) = \psi_0(0) \exp \left( (2k)^{-1} \int_0^r dr^0 [2 - V(r^0)] \sin 2[kr^0 + \psi_0(r^0)] \right) : \quad (6)$$

We then determine the corrective factor  $K$  from the amplitude function at large  $r$  using

$$K = \frac{\psi_0(r=0)^2}{\psi_0(r \rightarrow \infty)^2} : \quad (7)$$

In terms of the phase shift function  $\psi_0(r)$ , the corrective  $K$ -factor is given by

$$K = \exp \left( \frac{1}{k} \int_0^\infty dr^0 [2 - V(r^0)] \sin 2[kr^0 + \psi_0(r^0)] \right) : \quad (8)$$

It is convenient to express all radial distances in units of the Bohr radius

$$a_B = \frac{1}{j_e j} : \quad (9)$$

The Schrodinger equation in terms of  $x = r/a_B$  contains only the usual Coulomb parameter

$$= \frac{e}{v} \quad (10)$$

where  $v = k$  and  $j$  can be positive or negative, and the dimensionless screening length parameter

$$= \frac{D}{a_B} : \quad (11)$$

The  $K$ -factor is therefore only a function of  $j$  and  $D$ ; we shall show results for  $K(j, D)$  in the next section.

Note that the nonrelativistic energy  $E$  is equal to  $1 - (2 - a_B^2 j^2)$ , and the wave number  $k$  is equal to  $1 - (a_B j^2)$ ; thus,  $E$  and  $k$  decrease as  $j^2$  increases. In studying  $K(j, D)$  for the quark-gluon plasma, one can consider  $j^2$  a measure of the inverse of  $\overline{E}^P$  and  $D$  a measure of the inverse of the quark-gluon plasma temperature  $T$ .



### III. FEATURES OF THE CORRECTIVE FACTOR FOR SCREENED POTENTIALS

To illustrate some general features of the corrective factor  $K(k; a)$ , it is instructive to consider a simple potential similar to the screened potential (2), for which analytical corrective factor can be easily obtained. The truncated color-Coulomb potential  $V(r) = -\frac{g^2}{4\pi} \frac{e^{-\mu r}}{r}$  is qualitatively similar to the screened Yukawa potential (2), and can be chosen to match the Yukawa potential (2) with the same volume integral by setting  $a = \frac{p}{2\mu}$ . It can be shown easily that the corrective  $K$ -factor for this truncated color-Coulomb potential is

$$K = \frac{\sin(ka + \delta_0(a))^2}{F_0(k; ka)} \frac{2}{1 - \exp(-2g)}; \quad (12)$$

where  $\delta_0(a)$  is the phase shift for the truncated color-Coulomb potential  $V(r)$  and  $F_0(k; ka)$  is the usual regular s-wave Coulomb wave function (Eq. (14.1.3) of Ref. [39]).

For large values of  $a$  and  $ka \gg 1$ , we have  $\delta_0(a) = \ln(2ka) + \arg(1 - i)$  and

$$K = \frac{\sin \delta_0}{f \sin \delta_0 + g \cos \delta_0} \frac{2}{1 - \exp(-2g)}; \quad (13)$$

where

$$\delta_0 = ka + \ln(2ka) + \arg(1 - i); \quad (14)$$

and the asymptotic expansion of  $F_0(k; ka)$  gives [39]

$$f = 1 - \frac{5}{2ka} + \frac{5^2}{8k^2a^2}; \quad (15)$$

$$g = \frac{2}{2ka} - \frac{4^3}{8k^2a^2}; \quad (16)$$

The first factor on the righthand side of Eq. (13) is close to unity, with small oscillatory corrections. Therefore, for large values of  $a$  (which is proportional to  $\Lambda$ ),  $K(k; a)$  approaches and oscillates about the Gamow factor  $2 = (1 - \exp(-2g))$ , provided that  $ka$  is also large, corresponding to  $\Lambda \gg \mu$ .

For small values of  $a$  (or  $\lambda$ ) and  $ka$ , we can evaluate the phase shift  $\delta_0(a)$  in the Born approximation and obtain

$$\delta_0(a) = -k^2 a^2 (1 - k^2 a^2/6) : \quad (17)$$

From Eq. (12), an expansion of the Coulomb wave function in powers of  $ka$  leads to

$$K = \frac{[1 + ka(1 - k^2 a^2/6) - k^2 a^2/6]^2}{[1 - ka(2 - 1)k^2 a^2/6]^2} \frac{1 + 2 \frac{p}{2} \text{sign}(\epsilon)}{1 - 2 \frac{p}{2} \text{sign}(\epsilon)} ; \quad (18)$$

where  $\text{sign}(\epsilon)$  is the sign of  $\epsilon$ . By our convention in Eq. (2),  $\text{sign}(\epsilon) = 1$  for attractive  $q$ - $q$  interactions and  $\text{sign}(\epsilon) = -1$  for repulsive  $q$ - $q$  interactions. Therefore, for small values of  $\epsilon$  and small  $ka$  (which corresponds to  $|j| \gg 1$ ),  $K(\epsilon; \lambda)$  is approximately unity and is independent of  $|j|$ .

Having discussed the limiting behavior of  $K(\epsilon; \lambda)$ , we return to the screened color-Coulomb potential of Eq. (2) and display the corresponding corrective factor  $K(\epsilon; \lambda)$  as a function of  $\epsilon$  and  $\lambda$ . The corrective factor  $K(\epsilon; \lambda)$  for  $1 \leq \lambda \leq 1$  and  $\epsilon = 0.1; 0.2; \dots; 0.7$  is shown in Fig. 1. It is greater than unity for positive  $\epsilon$ , corresponding to an attractive interaction pulling the interacting particles together. It is less than unity for negative  $\epsilon$ , corresponding to a repulsive interaction pushing the interacting particles apart. For small  $\lambda$ , it approaches unity, indicating the diminishing influence of the interaction between the reacting particles for small screening lengths. The values of  $K(\epsilon; \lambda)$  for small  $\lambda$  and large  $\lambda$  agree with the estimates from Eq. (18).

We can also compare our results to the limit of no screening. It may be recalled that in this limit with  $\lambda \rightarrow 1$ , the corrective factor  $K(\epsilon; \lambda)$  approaches the Gamow factor which is only a function of  $\epsilon$ . The Gamow factor is shown in Fig. 1 as the dashed curve. For the range  $0 \leq \lambda \leq 1$  shown in Fig. 1,  $K(\epsilon; \lambda)$  increases as  $\epsilon$  and  $\lambda$  increase. It is quite close to the Gamow factor for  $\lambda > 0.7$ .

In Fig. 2 we show  $K(\epsilon; \lambda)$  as a function of  $\lambda$  in the range  $1 \leq \lambda \leq 3$  for various values of the screening length parameter  $\epsilon$ . The Gamow factor is the dashed curve. For small  $\epsilon$ ,

$K(\epsilon; \kappa)$  is nearly constant in  $\kappa$ . As the screening length parameter  $\epsilon$  increases, the corrective  $K$ -factor increases to become greater than the Gamow factor, reaches a maximum value, then reverses itself and oscillates about the Gamow factor. This oscillation about the Gamow factor can be understood from the approximate estimate of Eq. (13).

The peculiar behavior of the rise of  $K(\epsilon; \kappa)$  in the region of  $\epsilon \approx 1$  merits closer scrutiny. Accordingly, in Fig. 3a we study  $K(\epsilon; \kappa)$  as a function of  $\kappa$  in the range  $0.4 \leq \kappa \leq 2$ . We find that  $K(\epsilon; \kappa)$  is a maximum at  $\kappa = 0.835$ . The larger the values of  $\epsilon$ , the greater is the maximum value of  $K(\epsilon; \kappa)$ . The peak values of the  $K$ -factor are much greater than the corresponding Gamow factor, as indicated by the ratio  $K(\epsilon; \kappa)/(\text{Gamow factor})$  as a function of  $\kappa$  in Fig. 3b.

The prominent peak of  $K(\epsilon; \kappa)$  at  $\kappa = 0.835$  is due to the emergence of the lowest bound state of the system into the continuum to become a qq resonance as the screening length decreases. Movement of bound states into the continuum is familiar in the context of a single-particle system in a finite-range potential, as in the scattering of an electron from an atom [35,36]. An attractive screened potential with a large screening length is able to hold many negative-energy bound states. As an illustration, consider an attractive Coulomb potential which holds an infinite number of bound states. As the screening length  $\epsilon_D$  decreases from infinity, the Coulomb potential becomes a Yukawa potential with a decreasing range and its bound states are pushed into the continuum. Using semiclassical estimates, it has been noted that when the screening length is comparable to the Bohr radius, the screened potential cannot hold any bound state [9,2]. Numerical calculations show that

$0.84$  is the screening length parameter for which the lowest bound state in the screened potential becomes unbound [9]. This coincides with the location of the peaks of  $K(\epsilon; \kappa)$  in Fig. 3a. Combining the bound-state result of Ref. [9] with our continuum result for the  $K$ -factor, we conclude that the peak of the corrective factor at  $\kappa = 0.835$  arises because the lowest qq bound state emerges into the continuum to become a qq resonance as the screening length decreases. The occurrence of similar resonances for electron scattering from an atom has been observed earlier by Morse and collaborators [35,36].

There are other well-known physical phenomena in which bound states emerge into the continuum to become resonances as the range of the attractive potential decreases. For example, in nuclear physics the s-wave strength function obtained from very low energy neutron scattering shows peak values as a function of the nuclear mass number at  $A = 60$  and  $A = 160$ . (See page 230 of Ref. [40].) The s-wave strength function is related to the wave function at the nuclear surface, which is correlated with the wave function at the nuclear interior. The peaks of the s-wave strength function at  $A = 60$  and  $160$  correspond to the emergence of the bound single-particle  $4s_{1/2}$  and  $3s_{1/2}$  states respectively into the continuum as the nuclear mass number decreases. (See page 239 of Ref. [40].) The decrease of the nuclear mass number is accompanied by a decrease of the range of the attractive interaction. As a consequence, nucleon single-particle states are pushed into the continuum as the range of the interaction decreases, similar to the emergence of qq bound state into the continuum as the screening length decreases, as found in the present study.

The behavior of the qq resonance at  $\alpha = 0.835$  as a function of energy can be studied by examining the asymptotic phase shift  $(\delta_0 - \delta_0(r \rightarrow 1))$  for the screened potential as a function of  $E$  (in units of  $(2a_b^2)^{-1}$ ). For  $\alpha > 0.835$ , there is a bound state and the asymptotic phase shift  $\delta_0$  starts at  $\delta_0 = \pi$  at  $E = 0$  (according to Levinson's Theorem [41]), and  $\delta_0$  decreases monotonically as the energy increases (as in the short-dashed curve in Fig. 4). At  $\alpha = 0.835$ , the asymptotic phase shift starts at  $\delta_0 = 0$  at  $E = 0$ , rises to approximately  $\pi/2$ , and then decreases as the energy increases (the solid curve in Fig. 4). When  $\alpha < 0.835$ ,  $\delta_0$  rises from zero to a value close to  $\pi/2$  and decreases at higher energies. As  $\alpha$  decreases, the resonance peak (the location of the maximum  $\delta_0$ ) moves to higher energies, the maximum phase shift decreases, and the width of the structure increases. For  $\alpha < 0.835$ , although the phase shift nearly passes through  $\pi/2$  the corrective K-factor does not show a prominent peak structure at the resonance energy (the location of maximum  $\delta_0$ ), because the corrective K-factor is a rapidly decreasing function of the energy (approximately as  $1 = \frac{p}{E}$ ). The best indicator for the presence of this qq resonance at  $\alpha = 0.835$  appears to be the prominent peak structure of the corrective K-factor as a function of  $E$ , much as the manifestation of

s-wave resonances from the s-wave strength function plotted as a function of the nuclear radius or the nuclear mass number.

It is interesting to inquire whether there are similar peaks of  $K(\eta; \epsilon)$  at other locations of  $\epsilon$ . We have found that there is another similar peak of  $K(\eta; \epsilon)$  at  $\epsilon = 3.23$  (Fig. 5) corresponding to the second s-wave bound state emerging into the continuum to become a qq resonance. It is clear that other peaks of  $K$ -factor can occur at higher values of  $\epsilon$  when single-particle s-wave bound states are pushed into the continuum to become s-wave qq resonances as  $\mu_D$  decreases.

The  $K$ -factor for negative values of  $\epsilon$  gives the corrective factor for the lowest-order cross section involving two particles subject to a mutually repulsive screened interaction, as in the case of a  $q$  and a  $\bar{q}$  in color-octet states or two  $q^+$  particles subject to a screened Coulomb repulsion in pion interferometry. In Fig. 6 we show  $K(\eta; \epsilon)$  as a function of  $\epsilon$  in the range  $-3 \leq \epsilon \leq 0$  for different screening length parameters  $\mu_D = 0.1; 0.6; \dots; 3.1$ g. The corresponding Gamow factor (the no-screening limit) is also displayed. As one observes in this range of  $\epsilon$ , the  $K$ -factor for the screened potential is greater than the Gamow factor, and the deviation from the Gamow factor becomes greater, the larger is  $|\eta|$ . The screening length  $\mu_D$  need to be much greater than  $|\eta|$  to reach the no-screening limit. Thus, the effect of screening is also important for repulsive screened potentials, and the use of the Gamow factor for the case with screening may sometimes greatly over-correct the initial- or final-state interactions if  $\mu_D$  is small.

#### IV . CORRECTION FACTORS FOR TYPICAL PLASMA

In order to study the case of screening in the quark-gluon plasma, we make a minor modification to the general case examined in the last two sections. While we use the non-relativistic potential (2) to describe the interaction between a quark and an antiquark, we would like to include relativistic kinematics for the system, as we consider also kinetic energies with associated velocities of the order of 0.5. The use of relativistic kinematics

will avoid errors due to the neglect of the higher powers of the momentum, which would be present if we restricted ourselves to non-relativistic energy-momentum relations. In place of Eq. (1), the equation of motion to be solved is [31,42]

$$p^2 + b^2 - 2\epsilon A_0 = 0 \quad (19)$$

where  $A_0(r) = V(r)$ , and the quantities  $b$  and  $\epsilon$  can be expressed in terms of the center-of-mass energy  $\sqrt{s}$  as

$$\epsilon = (s - m_1^2 - m_2^2)/2\sqrt{s} \quad (20)$$

$$b^2 = [s^2 - 2s(m_1^2 + m_2^2) + (m_1^2 - m_2^2)^2]/4s = \frac{1}{4}\sqrt{s} m_w^2 \quad (21)$$

where  $m_w = m_1 m_2 / \sqrt{s}$ . The corresponding dimensionless parameters  $\eta$  and  $\alpha$  are

$$\eta = \frac{e}{v} = \frac{e\epsilon}{b} \quad (22)$$

and

$$\alpha = \frac{D}{a_B} = \frac{D}{\epsilon e\epsilon} : \quad (23)$$

Values of 1.5 GeV and 0.15 GeV have been used for the masses of the charm and strange quarks respectively.

The method outlined in Section III allows us to calculate the distortion corrections, which comprise the most important contribution to the  $K$ -factor at energies where the quark masses are not negligible. At this time we do not interpolate the  $K$ -factor to high-energy results involving radiative corrections; the finite temperature radiative corrections derived for the quark-gluon plasma [43,44] may be useful for this purpose.

For the quark-gluon plasma with a flavor number  $N_f$  and  $N_c = 3$ , lowest-order perturbative QCD gives a Debye screening length of [38]

$$\lambda_D(PQCD) = \frac{1}{\left(\frac{N_c}{3} + \frac{N_f}{6}\right)g^2 T} : \quad (24)$$

For a coupling constant  $\alpha_s = g^2/4 = 0.3$  and  $N_f = 3$ , the Debye screening length at a temperature of 200 MeV is  $r_D = 0.4$  fm. We examine the cases of  $r_D = 0.2$  and  $0.4$  fm, corresponding respectively to temperatures of 400 MeV and 200 MeV in this perturbative QCD estimate. We will calculate the associated K-factors for charm and strange pairs.

We show in Fig. 7a the corrective K-factor for  $c\bar{c}$  in a color-singlet state for which  $C_F = 4/3$  and  $K(\mu; \mu) > 1$ . For the  $c\bar{c}$  interaction, we use the running coupling constant [18,19]

$$\alpha_s(Q^2) = \frac{12}{(33 - 2N_f) \ln(Q^2/\Lambda^2)}; \quad (25)$$

and we assume four flavors and  $\Lambda_{QCD} = 300$  MeV. For  $r_D = 0.4$  fm, the K-factor is much greater than unity near the threshold of 3 GeV, and it decreases rapidly as a function of energy. The effective coupling constant is approximately  $\alpha_e = 0.4$  in this energy region, which gives a Bohr radius of  $a_B = 0.5$  fm. Thus, the screening length of  $r_D = 0.4$  fm corresponds to  $r_D/a_B = 0.8$ , which is near  $r_D/a_B = 0.835$  of peak K-factors, as we can infer from Fig. 3. The K-factor oscillates about the Gamow factor (the no-screening limit) which is shown as the dashed curve. It is much greater than unity near the threshold. For  $r_D = 0.2$  fm the K-factor is not as large. This corresponds to a value of  $r_D/a_B = 0.4$  for this energy region, far from  $r_D/a_B = 0.835$  where the peak of the K-factor is located.

We show in Fig. 7b the corrective K-factor for  $c\bar{c}$  in the color-octet state, for which  $C_F = 1/6$  and  $K(\mu; \mu) < 1$ . It decreases with increasing  $r_D$  and varies relatively smoothly with energy. The Gamow factor is also shown for comparison. The color-octet corrective factor is greater than the Gamow factor, and its deviation from unity is less than the deviation of the Gamow factor from unity.

Because the magnitude of the octet repulsive potential is less than the magnitude of the singlet attractive potential, the deviation of the K-factor from unity is greater for color-singlets than for color-octets.

We have extended our study to strange pair production or annihilation, as strange pair production is an important process in high-energy heavy-ion collisions which can be used as

a signature of a QGP. To study strangeness production in the quark-gluon plasma, we use the running coupling constant proposed by Godfrey and Isgur [45], which is appropriate for the energy range near the strange quark pair threshold:

$$\alpha_s(Q^2) = 0.25 \exp(-Q^2) + 0.15 \exp(-Q^2/10) + 0.2 \exp(-Q^2/1000); \quad (26)$$

where  $Q$  is in GeV. We display in Figures 8(a) and 8(b) the ss corrective  $K$ -factor in the presence of screening for color-singlets and color-octets respectively.

An interesting difference is observed in the color-singlet  $K$ -factors for charm and strange pairs near threshold for the same values for the screening length. For a charm quark pair, the corrective  $K$ -factor is larger than for a strange pair, and increases with decreasing energy. On the other hand, the color-singlet  $K$ -factor for strange quark pairs decreases slowly with decreasing energies. Both systems are studied at similar velocities as we are considering regions in which quark masses are important. Although the running coupling constants are different because the two systems sample different energy regions at threshold, this is not sufficient to account for the difference.

The difference in  $K(\beta; \gamma)$  for the charm and strange flavors in a similar velocity ranges can be understood in the light of the analysis in Section III. For screening lengths of 0.2 fm and 0.4 fm considered here, the values of  $\beta$  in the cc system are 0.4 and 0.8 respectively. The corresponding  $K(\beta; \gamma)$  have been discussed. For the ss system on the other hand, these values of  $\beta$  correspond to much smaller values of  $\gamma$ , due to the smaller mass of the strange quark. We find 0.04 and 0.08 for the two ss cases, and the deviation of  $K(\beta; \gamma)$  from unity is small. This is in accordance with the physical expectation that the interaction is suppressed when the range of the potential is small compared to the natural length scale of the system  $a_b$ , so the ss system responds almost as an unperturbed one.

## V. STRANGE AND CHARM QUARK-ANTIQUARK PRODUCTION

We now consider the effects of screening on cc and ss production cross sections near and above the threshold. The basic cross section for  $q\bar{q} \rightarrow g \rightarrow Q\bar{Q}$ , (where  $Q$  refers to s or c



quarks), averaged over initial and summed over final colors and spins can be written as [46]

$$\sigma_{q\bar{q}}(M_{Q\bar{Q}}) = \frac{8}{27} \frac{s^2}{M_{Q\bar{Q}}^2} \left( 1 + \frac{m}{2} \frac{1}{1 - m} \right); \quad (27)$$

where  $m = 4m_Q^2/M_{Q\bar{Q}}^2$ ,  $m_Q$  is the mass of the quark and  $M_{Q\bar{Q}}$  is the invariant mass of the produced  $Q\bar{Q}$  pair.

The corresponding expression for the gluon fusion mode, averaged over initial gluon types and polarizations and summed over final colors and spins is [46,2]

$$\sigma_{gg}(M_{Q\bar{Q}}) = \frac{s^2}{3M_{Q\bar{Q}}^2} \left( 1 + m + \frac{1}{16} m^2 \right) \ln \frac{1 + \frac{1}{1 - m}}{1 - \frac{1}{1 - m}} - \frac{7}{4} + \frac{31}{16} m \frac{1}{1 - m} : \quad (28)$$

To obtain the overall  $Q\bar{Q}$  (ss and cc) production, the above cross sections must be convoluted with the appropriate quark and gluon distributions. For charm and strange pair production in the quark-gluon plasma, these tree-level cross sections must be corrected to take into account the effect of Debye screening.

For  $Q\bar{Q}$  production by quark-antiquark annihilation through a virtual gluon mode at lowest order, the produced  $Q\bar{Q}$  pair is in a color-octet state. The corrective factor to be used is the color-octet corrective factor,  $K_{q\bar{q}} = K(\text{color octet})$  for the quark-gluon-plasma. The corrected cross-section is then

$$\sigma_{q\bar{q}}(M_{Q\bar{Q}}) = K_{q\bar{q}} \frac{8}{27} \frac{s^2}{M_{Q\bar{Q}}^2} \left( 1 + \frac{m}{2} \frac{1}{1 - m} \right); \quad (29)$$

In  $Q\bar{Q}$  production by gluon fusion,  $Q\bar{Q}$  pairs are produced with a relative color-octet and color-singlet population given by [25]

$$\frac{(\text{color octet})}{(\text{color singlet})} = \frac{(d^{abc} = \frac{1}{2})^2}{(f^{abc} = \frac{1}{3})^2} = \frac{5}{2} \quad (30)$$

Taking the weights of the population into account, we can write the corrective factor for the gluon fusion mode as  $K_{gg} = [5K(\text{octet}) + 2K(\text{singlet})] = 7$ . The cross-section for the gluon fusion production of  $Q\bar{Q}$  pairs, corrected for the effect of screening is then

$$\sigma_{gg}(M_{Q\bar{Q}}) = K_{gg} \frac{s^2}{3M_{Q\bar{Q}}^2} \left( 1 + m + \frac{1}{16} m^2 \right) \ln \frac{1 + \frac{1}{1 - m}}{1 - \frac{1}{1 - m}} - \frac{7}{4} + \frac{31}{16} m \frac{1}{1 - m} : \quad (31)$$

In Figures 9 and 10 we present the cross sections for  $c\bar{c}$  and  $s\bar{s}$  production corrected for screening effects in the quark-gluon plasma, together with the uncorrected cross sections for comparison. The cross sections for the case with the color-Coulomb interaction without screening are also shown. For  $s\bar{s}$  and  $c\bar{c}$  production by  $q\bar{q}$  annihilation, the intermediate virtual gluon selects color-octet states only. The color interaction is therefore repulsive and suppresses the cross section. With typical screening lengths of 0.2 and 0.4 fm, the corrected cross sections are near the no-screening color-Coulomb values for  $c\bar{c}$ , while for  $s\bar{s}$  production they are close to the tree level lowest-order values in accordance with the different values of  $\beta$  for the two flavors.

The gluon fusion modes on the other hand produce  $q\bar{q}$  pairs in a combination of color-singlet and color-octet states, and the larger magnitude of the color-singlet  $K$ -factor dominates the correction even though the singlet weight factor is lower. Here again, the cross sections for  $c\bar{c}$  production approach the no-screening color-Coulomb limit, whereas the cross sections for  $s\bar{s}$  production remain close to the lowest-order values, due to the differences in  $\beta$ . It may also be remarked that  $c\bar{c}$  production cross sections through the gluon fusion mode for  $\beta_D = 0.4$  fm exhibit a marked rise at small velocities caused by the maximum in the  $K$ -factor occurring as the lowest bound state emerges into the continuum at  $\beta = 0.835$ . On the other hand, the  $s\bar{s}$  production cross section is not appreciably affected by the corrective factors in the presence of screened fields. Distortion corrections in such a field are not expected to influence  $s\bar{s}$  cross sections in the plasma noticeably.

## V I. C O N C L U S I O N S A N D D I S C U S S I O N S

In reactions involving the production or the annihilation of a quark and an antiquark, the quark and the antiquark are subject to initial-state or final-state interactions due to their mutual interactions. The lowest-order cross sections for these processes can be corrected by using an approximate corrective  $K$ -factor to take into account the  $q$ - $\bar{q}$  interaction. In a deconfined quark-gluon plasma, the interaction between the quark and the antiquark is

screened. As a consequence, the corresponding  $K$ -factor will be modified. We have studied the effect of screening on the corrective  $K$ -factor. Our knowledge of such an effect can be used to search for the quark-gluon plasma. If the corrective  $K$ -factor can be inferred from experimental data, then we can use the relation between the color screening and the  $K$ -factor to deduce the conditions of screening and the possible presence of the deconfined phase of strongly-interacting matter.

In the present investigation we have limited our attention to energies near the  $q\bar{q}$  threshold, where the dominant contribution to the corrective  $K$ -factor comes from the distortion of the wave function by the  $q\bar{q}$  interaction which is modified by screening. The  $K$ -factors for the case with screening have been determined by numerical integration of the non-relativistic Schrodinger equation for  $q\bar{q}$  with a color-Yukawa potential. The  $K$ -factor gives an enhancement for color-singlet  $q\bar{q}$  states, due to the attractive nature of the color-singlet potential, but a suppression for color-octet  $q\bar{q}$  states due to the repulsive nature of the color-octet interaction. The color-singlet enhancement is larger in magnitude than the color-octet suppression because of the difference in the two strengths specified by the color factors of 4/3 and 1/6 respectively.

The corrective  $K$ -factor for the Yukawa interaction,  $\psi_e e^{-r/\lambda_D} = r$ , depends on two dimensionless parameters: the usual Coulomb' parameter  $\psi_e = v$ , and the screening length parameter  $\lambda_D = a_B$ . We have evaluated  $K(\psi_e; \lambda_D)$  for a large range of  $\psi_e$  and  $\lambda_D$ , to study how the  $K$ -factor depends on the  $q\bar{q}$  relative velocity and the screening length. The function  $K(\psi_e; \lambda_D)$  expressed in the dimensionless parameters  $\psi_e$  and  $\lambda_D$  can be used for other reactants interacting through a Yukawa potential.

For attractive Yukawa potentials we observe prominent peaks of the  $K$ -factor as a function of the screening length parameter  $\lambda_D$ . The peaks are located at  $\lambda_D = 0.835$  and  $\lambda_D = 3.23$ , corresponding to lowest two  $s$ -wave  $q\bar{q}$  bound states emerging into the continuum to become  $q\bar{q}$  resonances as the screening length decreases. These  $q\bar{q}$  resonances can be called "screening resonances" as they arise from the screening of the  $q\bar{q}$  interaction in the quark-gluon plasma. We have shown that their behavior is compatible with resonances expected for

potentials with finite range. This is also in accord with results obtained for the scattering of an electron from an atom [35,36], and is similar to the manifestation of resonances through the s-wave strength functions in low-energy neutron scattering from nuclei [40]. The explicit location of the peak at  $r_D = 0.835a_B$  coincides with the screening length at which the lowest qq state becomes unbound [9].

We have calculated the K-factors for two typical choices of the Debye screening length (0.2 fm and 0.4 fm), corresponding to plasma temperatures of approximately 400 and 200 MeV respectively. They are given separately for color-singlet and color-octet q-q states and can be used to correct the lowest-order cross sections. We have used these K-factors to investigate the effects of screening on the cross sections for charm and strange pair production. While the corrections to the cross section in the no-screening color-Coulomb limit are of similar magnitude for ss and cc pairs in the same velocity range, they are considerably different for the two systems in the presence of screening with a color-Yukawa interaction. This arises because the Bohr radius is much smaller for the c-c system than for the s-s system. A screening length of 0.4 fm would correspond to  $r_D = 0.8$  for c-c but only 0.08 for s-s. The screening length parameter  $r_D = 0.8$  happens also to be near the location where a c-c resonance occurs at  $E = 0$ . Thus, c-c color singlet production is much enhanced for  $r_D = 0.4$  fm. There is no such enhancement for s-s production at this screening length.

Since the single virtual gluon in qq annihilation leads to color octet pair production, the lowest order rates for  $qq \rightarrow cc(ss)$  are larger than the corrected ones because the octet correction is suppressive. On the other hand, qq production by gluon fusion can proceed through color-singlet or octet states, the weight being given by  $2=5$  for singlet to octet. Despite the lower weight, the larger magnitude of the color-singlet K-factor results in the attractive potential dominating, so that the net effect of the correction is an enhancement of gluon fusion production.

It is also noteworthy that the peak of the K-factor in the cc system corresponds to the unbinding of the lowest bound state and its emergence as a cc resonance. It is manifested as a rise in the gluon fusion cross sections near threshold, for a screening length of 0.4 fm,

which is near the screening length required for a peak in the  $K$ -factor, as shown in Fig. 9. Gluon fusion being the dominant mode for heavy-quark production, the combined effect is to have a peak in the  $c\bar{c}$  production cross section just above the  $c\bar{c}$  threshold, with a relatively narrow width in energy. Thus, the occurrence of a  $c\bar{c}$  resonance will be signalled by a large enhancement of  $c\bar{c}$  production just above the threshold. This is in contrast to  $s\bar{s}$  production for  $r_D = 0.2 - 0.4$  fm, for which the corresponding screening length parameters of  $r_D = 0.04 - 0.08$  are very small and are far from  $r_D = 0.835$  for a  $q\bar{q}$  resonance.

From our results, the occurrence of  $q\bar{q}$  screening resonances may provide a way to search for the quark-gluon plasma. The  $q\bar{q}$  resonances give rise to prominent peaks of the  $K$ -factor as a function of the screening length parameter, which is the ratio of the screening length  $r_D$  to the Bohr radius  $a_B$ . The screening length is inversely proportional to the temperature [38]. Thus,  $q\bar{q}$  resonances lead to prominent peaks of the  $K$ -factor as a function of the plasma temperature. We have seen in Fig. 9 that large values of the  $K$ -factor near the threshold give rise a narrow peak in the heavy-quark production cross section just above the threshold. The occurrence of a  $q\bar{q}$  resonance will be accompanied by a much enhanced  $q\bar{q}$  production cross section just above the threshold, and the enhancement will be a function of the temperature.

The search for  $q\bar{q}$  screening resonances in the quark-gluon plasma can make use of the peaks of the  $K$ -factor at  $r_D = 0.835$  and  $r_D = 3.23$ . The resonance at  $r_D = 3.23$  may not lead to realizable enhancements because it corresponds to temperatures much below the estimated quark-gluon plasma transition temperature (of approximately 150 - 200 MeV). Using the perturbative QCD estimates, the screening length parameter of  $r_D = 0.835$  corresponds to a  $c\bar{c}$  resonance at  $T_{c\bar{c}} = 165$  MeV and a  $b\bar{b}$  resonance at  $T_{b\bar{b}} = 393$  MeV. These  $T_{c\bar{c}}$  and  $T_{b\bar{b}}$  estimates from PQCD are approximate and uncertain, as lattice gauge theory gives Debye screening lengths of about half of PQCD estimates. (See Fig. 7 of [47].) The Debye screening length needs to be determined by experimental searches for these  $c\bar{c}$  and  $b\bar{b}$  resonances using the peaks in the  $K$ -factors. The PQCD estimates are useful only as a rough guide. Thus, for  $T = T_{c\bar{c}}$  (approximately 165 MeV), and if the quark-gluon plasma is produced,

$(cc) = 0.835$  and there will be a large enhancement of  $cc$  production near the threshold, much greater than what one expects from the lowest-order cross sections (Fig. 3). At temperatures far from the  $cc$  resonance temperature  $T_{cc}$  there is no such large enhancement of  $cc$  production near threshold. At  $T = T_{bb}$  (approximately 393 MeV), if the quark-gluon plasma is produced,  $(bb) = 0.835$  and there will be a large enhancement of  $bb$  production near the threshold, again much greater than expected from the lowest-order cross sections. At temperatures far from the  $bb$  resonance temperature  $T_{bb}$ , there is no such large enhancement of  $bb$  production near the thresholds. Temperature dependence of this type arises from the nature of screening between the interacting heavy quark and its antiquark partner, which is an important property to identify the deconfined quark-gluon plasma. A search for the quark-gluon plasma using heavy-quark resonances will require the measurement of the production yield of heavy-quark pairs near the threshold, and a method to estimate the temperature of the environment in which the production takes place. The enhancement will occur either for the production of heavy-quark pairs by the collision of the constituents of the thermalized quark-gluon plasma, or by the collision of the partons in nucleon-nucleon collisions in a quark-gluon plasma environment.

It is interesting to note the recent report from the NA 38 and the Helios-3 Collaborations of an excess of dileptons at a dilepton invariant mass of 1.5 to 2.5 GeV [48{50]. The NA 38 Collaboration suggests that this may be due to an excess production of charm pairs in high-energy nucleus-nucleus collisions [49]. The estimate from our work gives  $cc$  screening resonance occurring at a temperature  $T_{cc}$  about 165 MeV, which is within the experimental range of temperatures as encountered in the NA 38 and the Helios-3 experiments. It will be of great interest to have a direct measurement of charm pair production near the threshold for the reactions studied by NA 38 and Helios-3, to see whether there are indeed excess charm pairs near the threshold, and whether these excess charm pairs arise as a manifestation of a  $cc$  resonance emerging just above the threshold in a quark-gluon plasma, or from some other processes [15].

After the work in the present paper was completed, a recent study of the effect of a re-

pulsive screened Coulomb interaction between two pions in pion interferometry was brought to our attention [51]. The modification of the Gamow factor due to screening was obtained in [51] by using a quasi-classical approximation to barrier penetration, whereas the results obtained here (Section III) for repulsive screening potential follow from exact integration of the Schrodinger equation. For this special case of a repulsive screened potential, our exact results complement the quasi-classical approximate solutions of [51].

## VII. ACKNOWLEDGEMENTS

The authors would like to thank Dr. Ray Satchler, ORNL, for valuable discussions. Lali Chatterjee would like to thank Dr. Anand K. Bhatia, NASA, Goddard Space Flight Center for helpful discussions, and Dr. M. Strayer and Dr. F. Plasil for their kind hospitality at ORNL. This research was supported in part by the Division of Nuclear Physics, U.S. Department of Energy under Contract No. DE-AC05-96OR22464, managed by Lockheed Martin Energy Research Corp.

## REFERENCES

<sup>y</sup> On leave from Department of Physics, Jadavpur University, Calcutta 700032, India.

- [1] Proceedings of Quark Matter 95, at Monterey, California, published in Nucl. Phys. A 590, 1995.
- [2] C. Y. Wong, Introduction to High-Energy Heavy-Ion Collisions, World Scientific Publishing Company, 1994.
- [3] E. V. Shuryak, The QCD Vacuum, Hadrons and the Superdense matter, World Scientific Publishing Company, 1988.
- [4] H. Satz, Zeit. Phys. C 62, 683 (1994).
- [5] B. Muller, Nucl. Phys. A 590, 3c (1995); M. Gyulassy, Nucl. Phys. A 590, 431c (1995).
- [6] J. W. Harris and B. Muller, hep-ph/9602235.
- [7] J. Stachel and G. R. Young, Ann. Rev. Part. Phys. 42, 537 (1992).
- [8] T. Matsui and H. Satz, Phys. Lett. B 178, 416 (1986).
- [9] T. Matsui, Zeit. Phys. C 38, 245 (1988).
- [10] F. Karsch and H. W. W. yld, Phys. Lett. B 213, 505 (1988).
- [11] J. D. Bjorken, Phys. Rev. D 27, 140 (1983).
- [12] E. Shuryak and L. Xiong, Phys. Rev. Lett. 70, 2241 (1993); E. Shuryak, Nucl. Phys. A 566, 559 (1994).
- [13] J. I. Kapusta, Nucl. Phys. A 566, 45c (1994).
- [14] C. Y. Wong, Phys. Rev. Lett. 76, 196 (1996).
- [15] C. Y. Wong, Phys. Lett. B 367, 50 (1996).
- [16] J. Kubar, M. Le Bellac, J. L. Mounier, and G. Plaut, Nucl. Phys. B 175, 251 (1980).



- [17] R. Hamberg, W. L. van Neerven, and T. Matsuura, Nucl. Phys. B 359, 343 (1991).
- [18] R. D. Field, Applications of Perturbative QCD, Addison-Wesley Publishing Company, 1989.
- [19] R. Brock et al.; Handbook of Perturbative QCD, (CTEQ Collaboration), Editor George Sterman, Fermilab Report, Fermilab-pub-93/094, 1993.
- [20] C. Grosso-Pilcher and M. J. Shochet, Ann. Rev. Nucl. Part. Sci. 36, 1 (1986).
- [21] T. Applequist and H. D. Polizer, Phys. Rev. Lett. 34, 43 (1975); Phys. Rev. D 12, 1404 (1975).
- [22] R. M. Barnett, M. Dine, and L. McLerran, Phys. Rev. D 22, 594 (1980).
- [23] S. Gusken, J. H. Kuhn, and P. M. Zerwas, Phys. Lett. 155B, 185 (1988).
- [24] V. Fadin and V. Khoze, Soviet Jour. Nucl. Phys. 48, 487 (1988).
- [25] V. Fadin, V. Khoze, and T. Sjstrand, Zeit. Phys. C 48, 613 (1990).
- [26] S. J. Brodsky, A. H. Hoang, J. H. Kuhn and T. Teubner, hep-ph/9508274.
- [27] G. Gamow, Zeit. Phys. 51, 204 (1928), see also L. I. Schiff, Quantum Mechanics, McGraw-Hill Company, 1955, p. 142. A. Sommerfeld, Atombau und Spektrallinien, Bd. 2. Braunschweig: Vieweg 1939.
- [28] M. Gyulassy and S. K. Kaufmann, Nucl. Phys. A 362 (1981) 503.
- [29] I. Harris and L. M. Brown, Phys. Rev. 195, 1656 (1957).
- [30] H. A. Bethe and P. Morrison, Elementary Nuclear Theory, John Wiley and Sons, New York, 1956; J. M. Blatt and V. F. Weisskopf, Theoretical Nuclear Physics, John Wiley and Sons, New York, 1952, p. 731.
- [31] L. Chatterjee and C. Y. Wong, Phys. Rev. C 51, 2125 (1995).

- [32] J. Schwinger, *Particles, Sources, and Fields* (Addison-Wesley, New York, 1973), Vol. II, Chaps. 4 and 5.
- [33] M. G. H. Mostafa, C. Y. Wong, Lali Chatterjee, Zhong-Qi Wang, hep-ph/9503357, *Int. Jour. Mod. Phys.* (in press).
- [34] L. Chatterjee and C. Y. Wong, hep-ph/9501218.
- [35] P. M. Morse, *Rev. Mod. Phys.* 4, 577 (1932).
- [36] W. P. Allis and P. M. Morse, *Zeit. Phys.* 70, 567 (1931).
- [37] F. Calogero, *Variable Phase Approach to Potential Scattering*, Academic Press, N.Y. 1967.
- [38] D. Gross, R. D. Pisarski, and L. G. Ya e, *Rev. Mod. Phys.* 53, 43 (1981).
- [39] M. Abramowitz and I. Stegun, *Handbook of Mathematical Functions*, Dover Publications, N.Y., 1965.
- [40] A. Bohr, and B. Mottelson, *Nuclear Structure*, W. A. Benjamin, Inc., New York, 1967.
- [41] N. Levinson, *Kgl. Danske Videnskab., Mat. fys. Medd.* 25, No. 9, 1949).
- [42] H. W. Crater, R. Becker, C. Y. Wong and P. van Alstine, *Phys. Rev. D* 46, 5117 (1992);  
H. W. Crater, R. Becker, C. Y. Wong and P. van Alstine, Oak Ridge National Report, No. ORNL/TM-12122, 1992 (unpublished).
- [43] E. Braaten and R. D. Pisarski, *Nucl. Phys. B* 337, 569 (1990).
- [44] T. A. Therr, P. Aurenche, and T. Bechereray, *Nucl. Phys. B* 315, 436 (1989); T. A. Therr and V. Ruuskanen, *Nucl. Phys. B* 380, 377 (1989); T. A. Therr and V. Ruuskanen, *Nucl. Phys. B* 380, 377 (1992).
- [45] S. Godfrey and N. Isgur, *Phys. Rev. D* 32, 189, (1985).
- [46] B. L. Combridge, *Nucl. Phys. B* 151, 429 (1979).

- [47] A. Ukawa, Nucl. Phys. A 498, 227c (1989).
- [48] C. Lourenco, Proc. of the Hirschegg '95 Workshop, 'Hadrons in Nuclear Matter', Hirschegg, Austria, 1995 (Ed. GSI); CERN Report CERN-PPE/95-72, 1995 (LIP Preprint 95-03, 1995).
- [49] S. Ramos, NA 38 Collaboration, Nucl. Phys. A 566, 77c (1994); M. C. Abreu et al., NA 38 Collaboration, Nucl. Phys. A 566, 77c (1994).
- [50] M. Maseara, HELIOS-3 Collaboration, Nucl. Phys. A 590, 93c (1995); M. A. Mazzoni, HELIOS-3 Collaboration, Nucl. Phys. A 566, 95c (1994).
- [51] D. V. Anichkin, W. A. Zajc, and G. M. Zinovjev, hep-ph/9512279.

## FIGURES

FIG .1. The corrective factor  $K(\mu; \lambda)$  plotted as a function of  $\mu$  for different values of the dimensionless screening parameter  $\lambda$ . The parameter  $\lambda$  is positive for an attractive Yukawa potential and is negative for a repulsive Yukawa potential. The Gamow factor for the case of Coulomb (or color-Coulomb) interaction is also shown as the dashed curve.

FIG .2. The corrective factor  $K(\mu; \lambda)$  plotted as a function of  $\mu$  for  $\lambda = 1, 3$  and various values of  $\mu$ . The Gamow factor for the case of Coulomb interaction is also shown as the dashed curve.

FIG .3. (a) The corrective factor  $K(\mu; \lambda)$  plotted as a function of  $\mu$  for  $\lambda = 0.4, 2$  and different values of  $\mu$ , (b) the ratio  $K(\mu; \lambda)/(\text{Gamow factor})$  as a function  $\mu$  for different values of  $\lambda$ .

FIG .4. The phase shift  $\delta_0$  as a function of energy for  $\lambda$  near 0.835.

FIG .5. (a) The corrective factor  $K(\mu; \lambda)$  plotted as a function of  $\mu$  for  $\lambda = 1.5, 5.0$  and different values of  $\mu$ , (b) the ratio  $K(\mu; \lambda)/(\text{Gamow factor})$  as a function  $\mu$  for different values of  $\lambda$ .

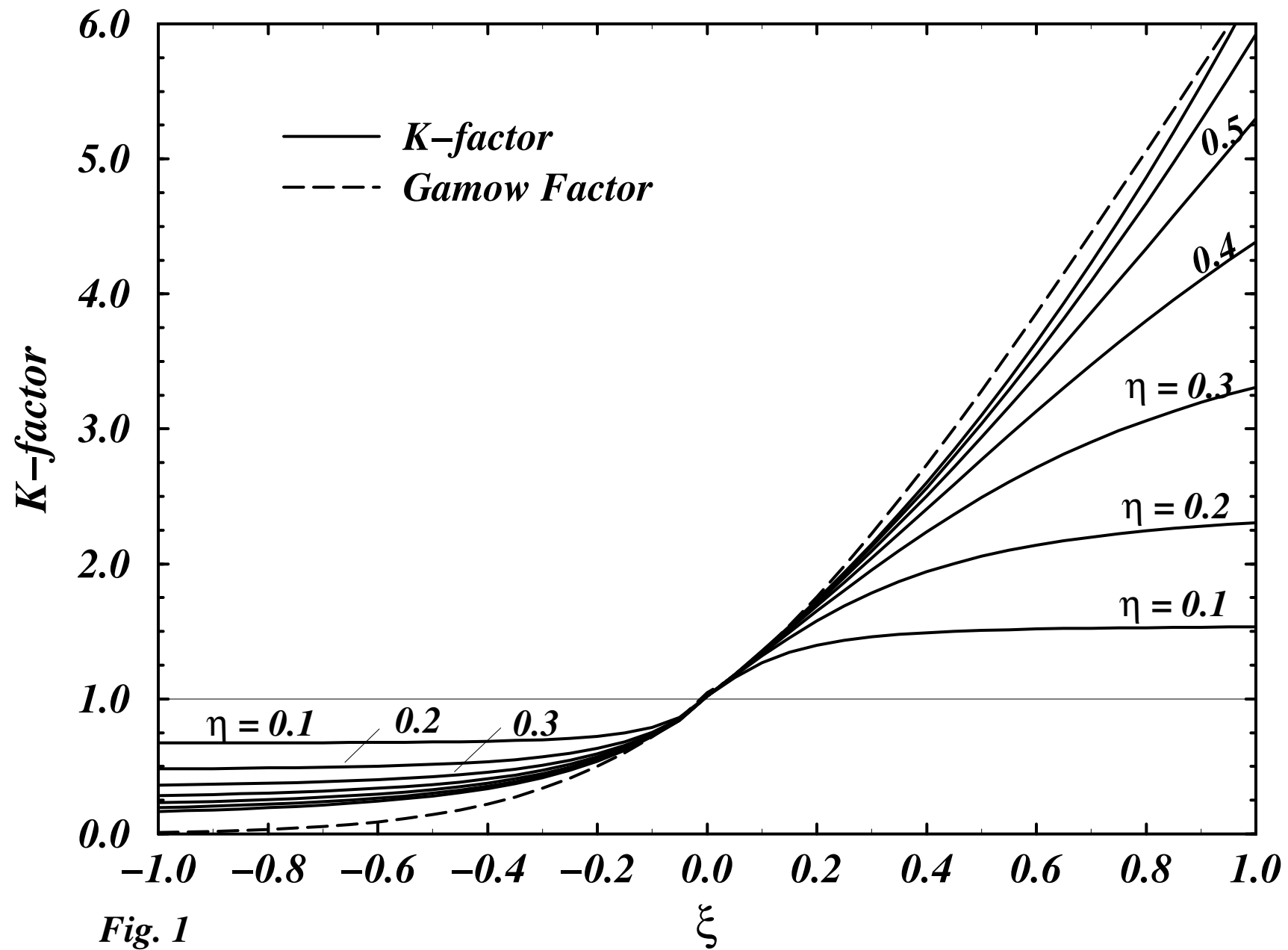
FIG .6. (a) The corrective factor  $K(\mu; \lambda)$  plotted as a function of  $\mu$  for  $\lambda = 3, 0$  and different values of  $\mu$ . Negative values of  $\lambda$  represent a repulsive Yukawa interaction. The Gamow factor for the case of Coulomb interaction is shown as the dashed curve. (b) the ratio  $K(\mu; \lambda)/(\text{Gamow factor})$  as a function  $\mu$  for different values of  $\lambda$ .

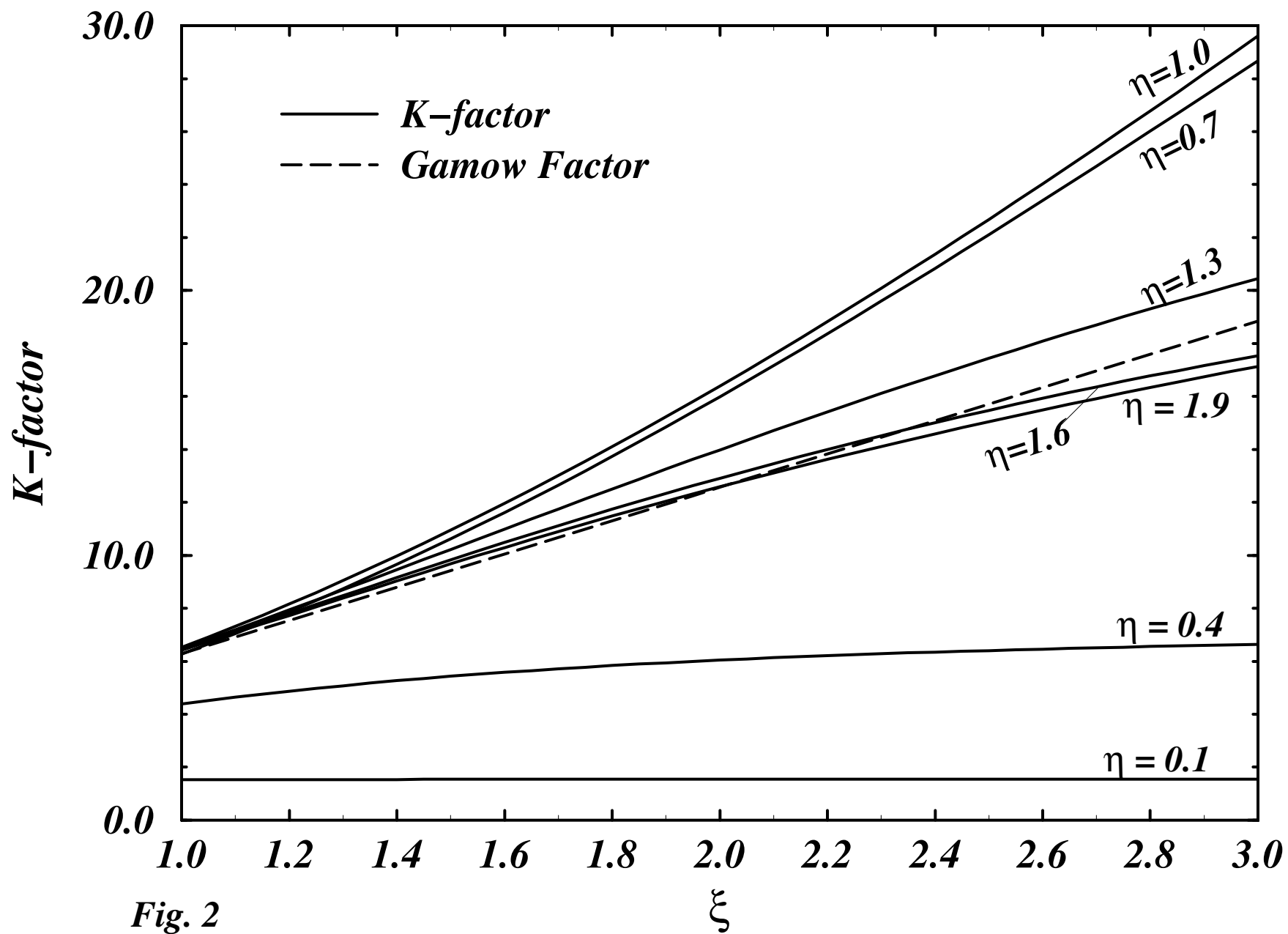
FIG .7. The corrective factor  $K(\mu; \lambda)$  for a cc pair with screening length  $\lambda_D = 0.2$  and  $0.4 \text{ fm}$ , as a function of the center-of-mass energy  $\sqrt{s}$ . The Gamow factor is shown as a dashed curve for comparison. Fig. 7 (a) is for color-singlet cc states, and Fig. 7 (b) is for color-octet cc states.

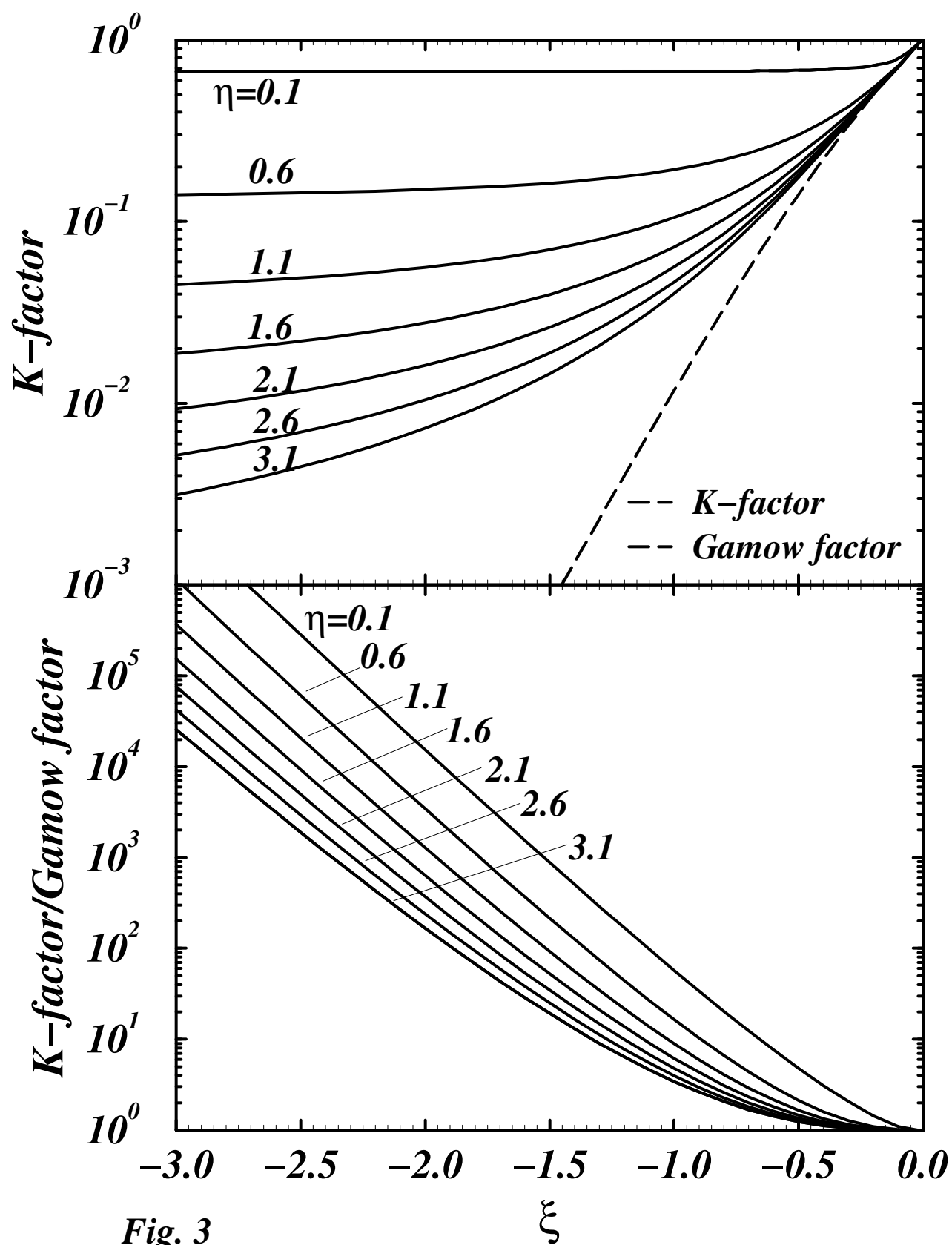
FIG .8. The corrective factor  $K(\mu; \lambda)$  for an ss pair with screening length  $\lambda_D = 0.2$  and  $0.4 \text{ fm}$ , as a function of the center-of-mass energy  $\sqrt{s}$ . The Gamow factor is shown as a dashed curve for comparison. Fig. 8 (a) is for color-singlet ss states, and Fig. 8 (b) is for color-octet ss states.

FIG. 9. Cross sections for  $c\bar{c}$  production (a) by gluon fusion, and (b) by  $q\bar{q}$  annihilation, with screening lengths of  $r_D = 0.2$  and  $0.4$  fm. The lowest-order cross section and the cross section in the case of color-Coulomb  $c\bar{c}$  interaction are also shown.

FIG. 10. Cross sections for  $s\bar{s}$  production (a) by gluon fusion, and (b) by  $q\bar{q}$  annihilation, with screening lengths of  $r_D = 0.2$  and  $0.4$  fm. The lowest-order cross section and the cross section in the case of color-Coulomb  $s\bar{s}$  interactions are also shown.









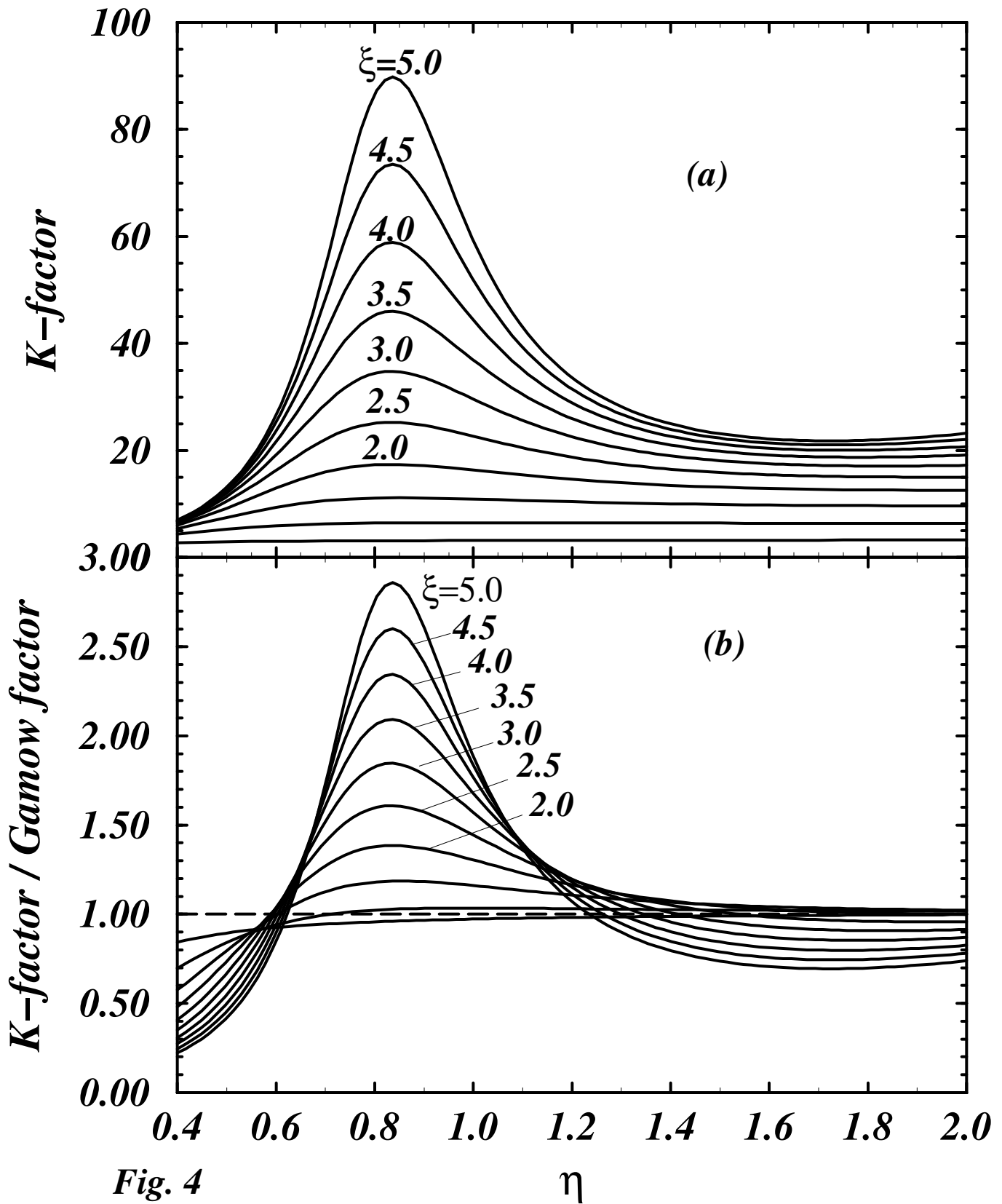
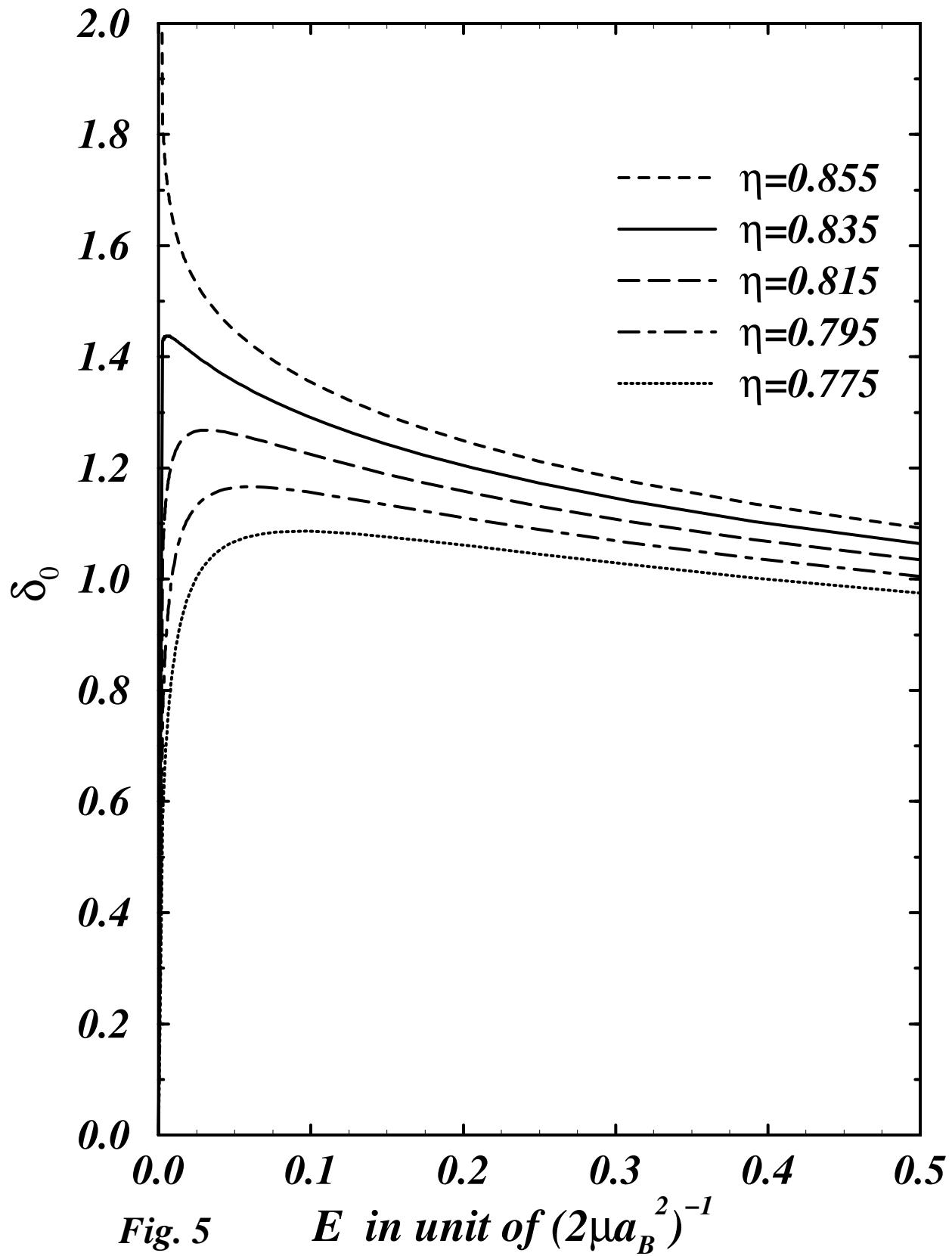


Fig. 4



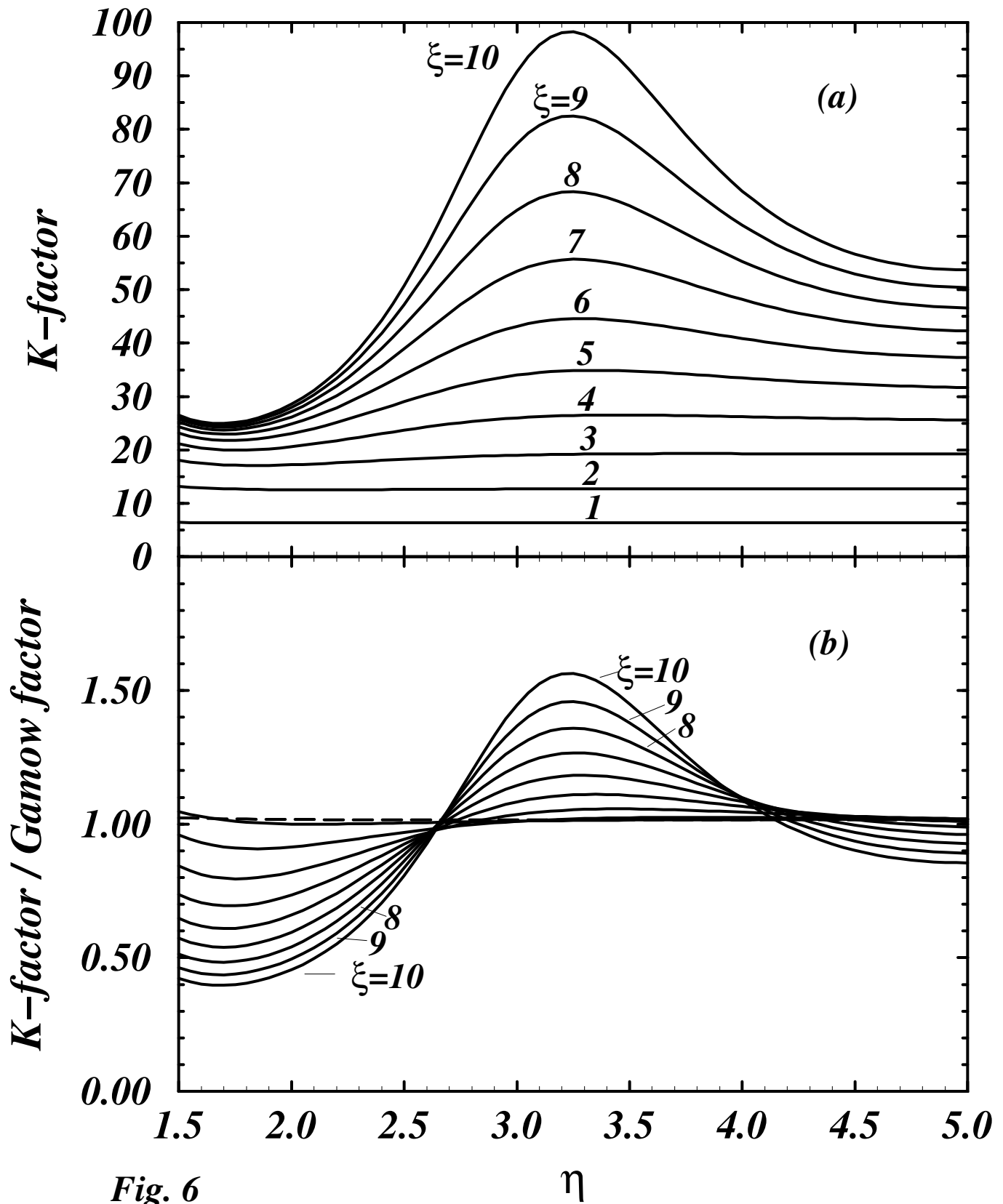
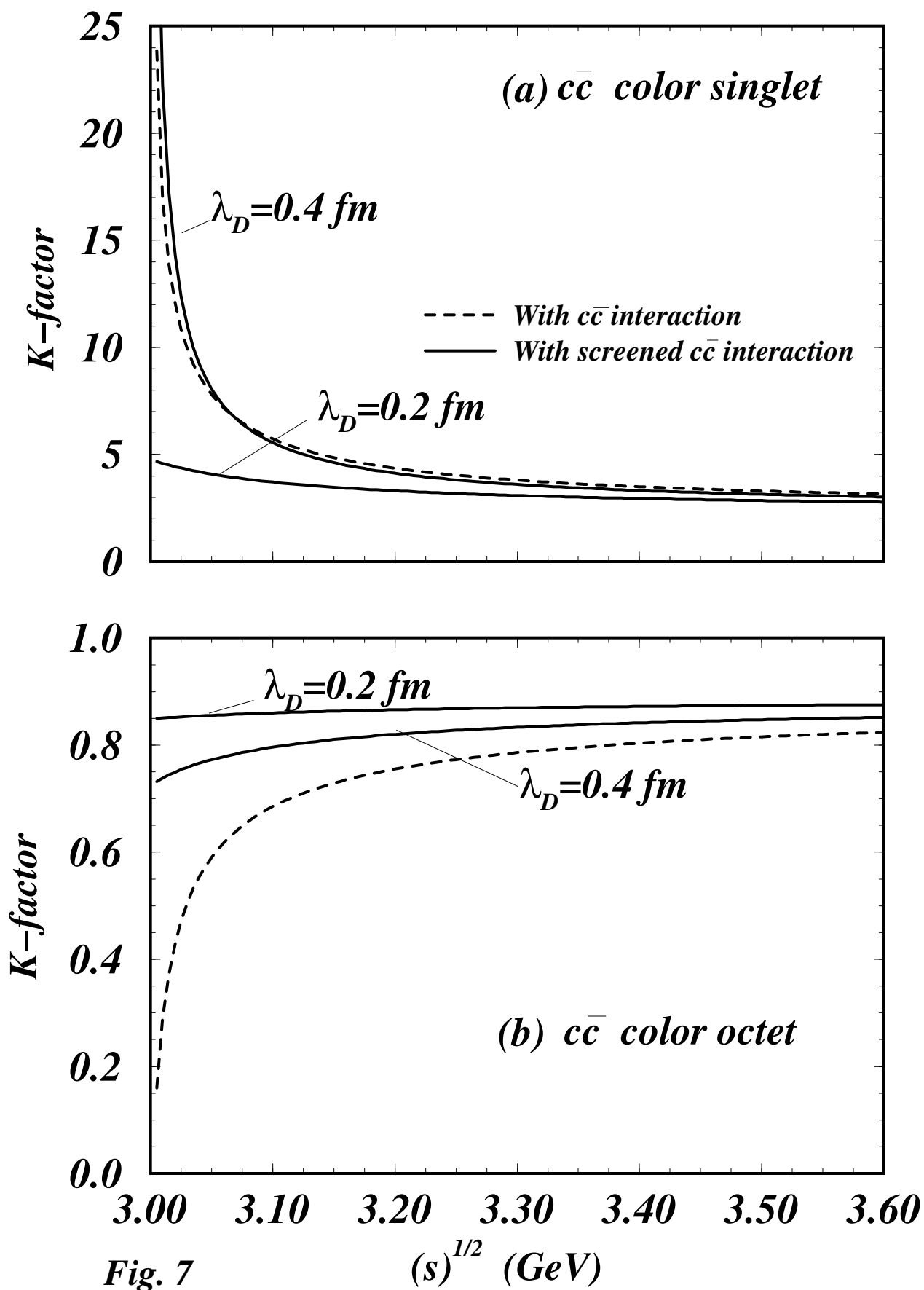
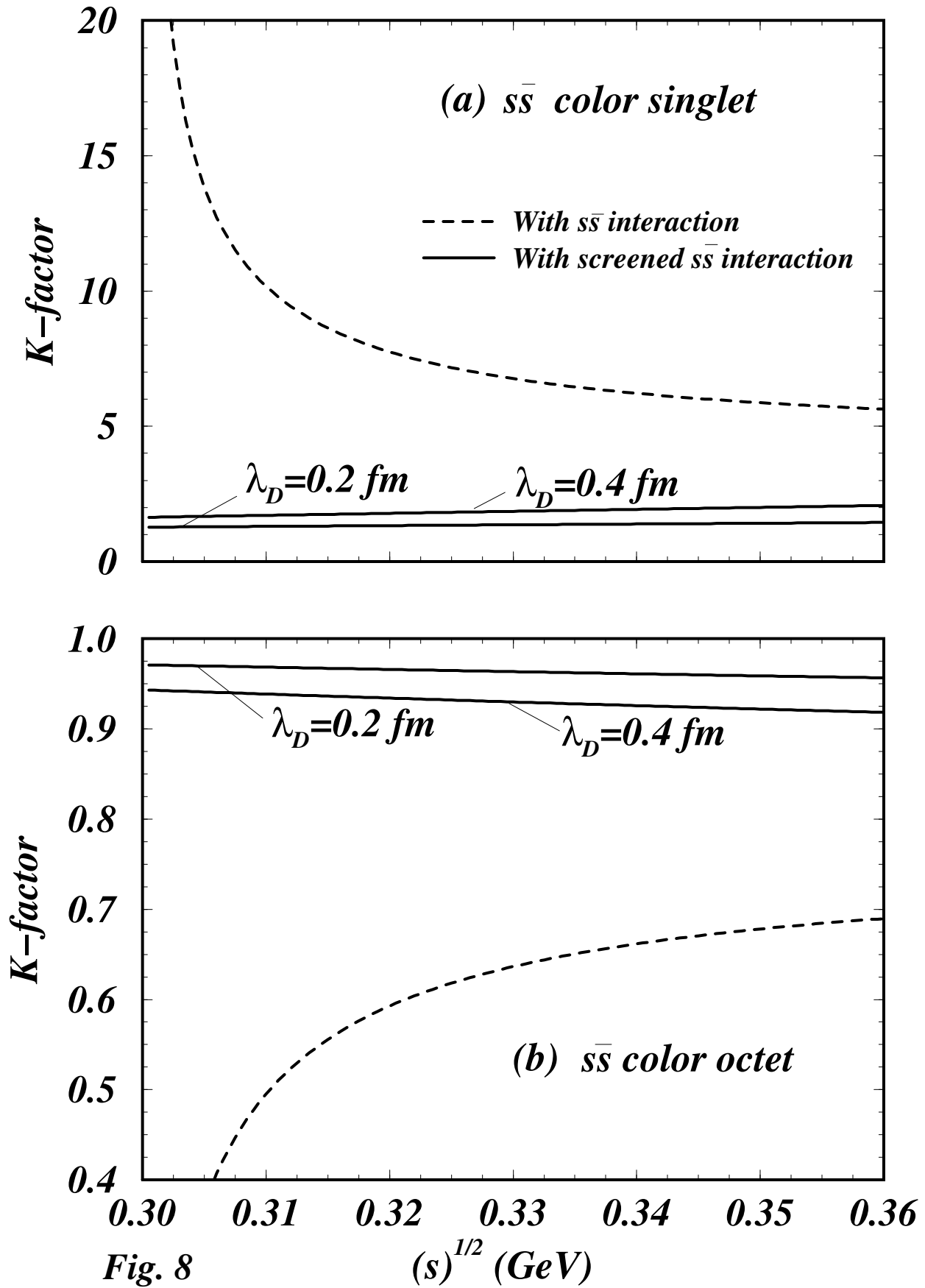


Fig. 6





**Fig. 8**

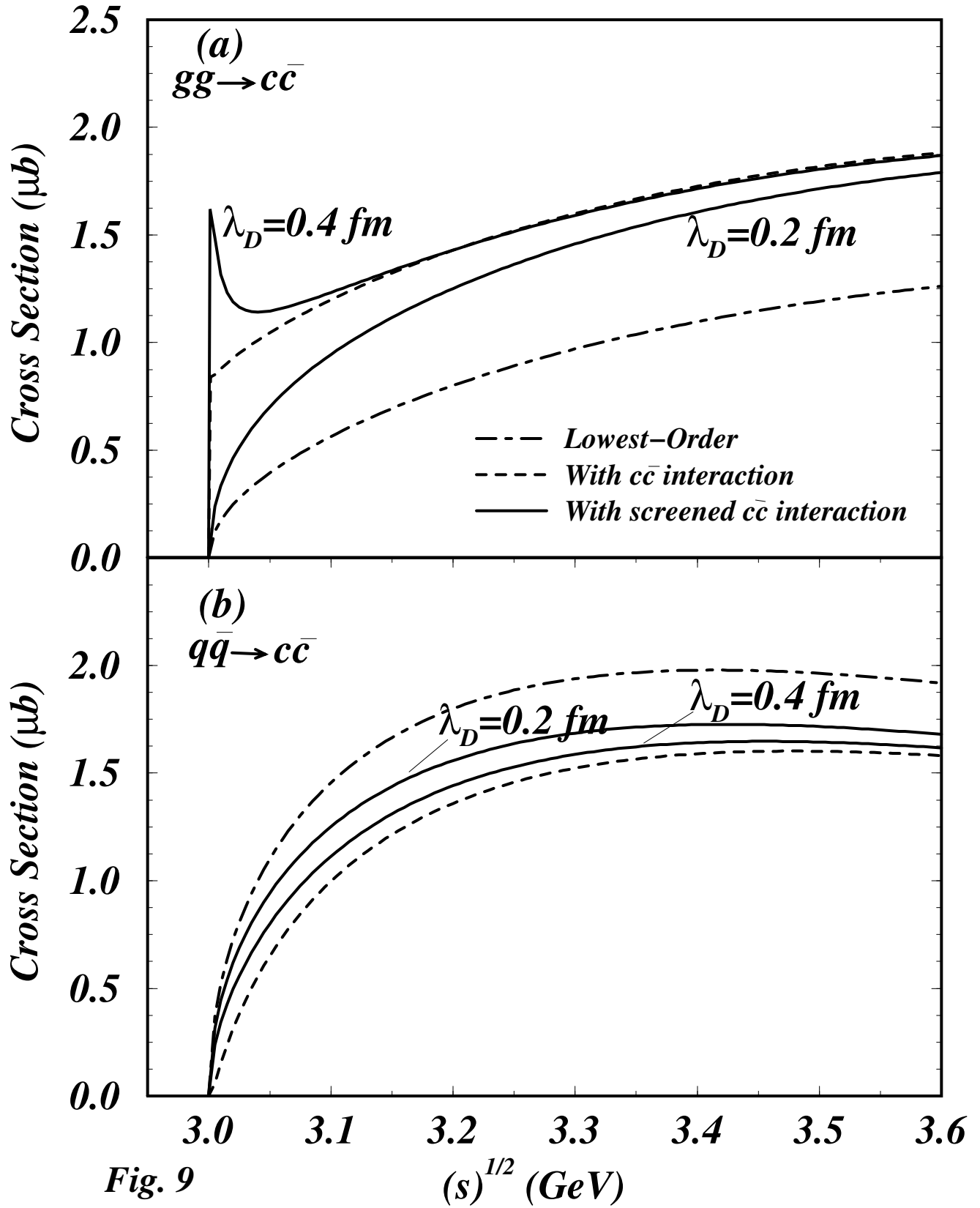
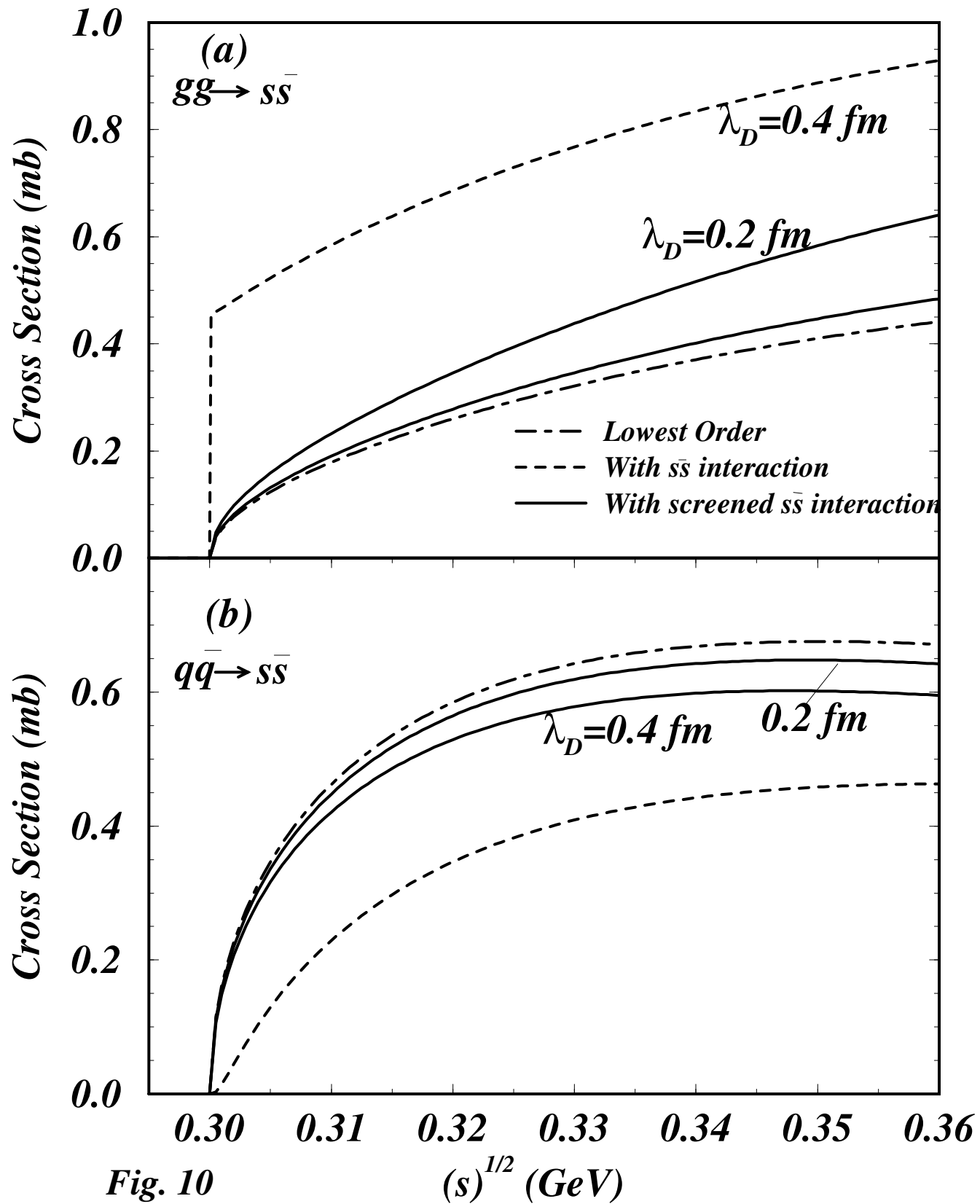


Fig. 9



**Fig. 10**